Robust Regenerator Allocation in Nonlinear Flexible-Grid Optical Networks With Time-Varying Data Rates

Li Yan, Yuxin Xu, Maïté Brandt-Pearce, Nishan Dharmaweera, and Erik Agrell

***Abstract*—Predeployment of regenerators in a selected subset of network nodes allows service providers to achieve rapid provisioning of traffic demands, high utilization, and reduced network operational costs, while still guaranteeing lightpath quality of transmission. Enabled by bandwidth-variable transceivers in flexible-grid optical networks, optical channel bandwidths are no longer fixed but constantly changing according to real-time communication requirements. Consequently, the data-rate-variable traffic together with other new network features introduced by flexible-grid networks will render the regenerator allocation very difficult due to the complicated network states. In this paper, we investigate how to allocate regenerators robustly in flexible-grid optical networks to combat physical-layer impairments when the data rates of traffic demands are random variables. The Gaussian noise model and a modified statistical network assessment process framework are used to characterize the probabilistic distributions of physical-layer impairments for each demand, based on which a heuristic algorithm is proposed to select a set of regenerator sites with minimum blocking probabilities. Our method achieves the same blocking probabilities with on average 10% less regenerator sites compared with the greedy constrained-routing regenerator allocation method, and obtains blocking probabilities two orders of magnitude lower than that of the routing and reach method with the same number of regenerator sites.**

***Index Terms*—Network optimization; Physical-layer impairments; Regenerator placement; Variable traffic.**

I. Introduction

The rapid rise in the use of mobile Internet, video streaming, and cloud computing services has led to increasing data volumes and diversified traffic requests, which put severe pressure on backbone optical networks. Flexible-grid optical networks have been proposed to relax the rigid spectrum grid requirement of wavelength-division multiplexing (WDM) networks and offer much higher efficiency by adaptively assigning spectrum to traffic demands [1].

Moreover, new network and transmission techniques are also introduced to further improve the network capacity. Enabled by bandwidth-variable wavelength cross-connects (BV-WXCs) and bandwidth-variable transceivers (BV-Ts) [2], network operators can dynamically change the bandwidths of optical channels according to real-time communication requirements and thus, achieve cost-effective and highly available connectivity services. For example, data centers may require more bandwidth from the network for data backup during night hours. The video-on-demand services of individual users are usually high during evening hours, and a large amount of inter-office traffic of enterprises is transported during the business hours [2,3]. During hours of low bandwidth requirements, the unused resources are then released and assigned to other network services. Additionally, the advent of higher-order modulation formats and variable coding-rate schemes [4–6] will allow finer granularity of spectrum efficiency in transmission systems. Consequently, the state of the network[1] becomes extremely complicated and physical-layer impairments (PLIs) will be the dominant limitation for satisfactory lightpath quality of transmission (QoT) and optical reach.

To achieve long-haul transmission between nodes in flexible-grid optical networks, one or more optoelectronic regenerators may have to be used to restore optical signals. However, each regenerator adds a cost comparable to a pair of endpoint transceivers [7], requiring the system operators to predeploy them as efficiently as possible. By deploying regenerators at a subset of the network nodes, referred to as regenerator sites (RSs), we can achieve better sharing of spare regenerators for randomly variable demands and improve operational efficiency by requiring fewer truck rolls [8], which require dispatching technicians in a truck to install or maintain the network equipment.

The problem of allocating a set of RSs is described as the regenerator location problem (RLP), which has been proven to be non-deterministic polynomial-time hard (NP-hard) [9,10] when routes are not specified for each source–destination pair. The authors of [9] also propose

Manuscript received March 23, 2018; revised July 28, 2018; accepted July 30, 2018; published September 4, 2018 (Doc. ID 326742).

L. Yan (e-mail: lyaa@chalmers.se) and E. Agrell are with Chalmers University of Technology, Gothenburg SE-41296, Sweden.

Y. Xu and M. Brandt-Pearce are with University of Virginia, Charlottesville, Virginia 22904, USA.

N. Dharmaweera is with the Department of Electrical and Electronic Engineering, University of Sri Jayewardenepura, Nugegoda 10100, Sri Lanka.

https://doi.org/10.1364/JOCN.10.000823

[1]In this paper, the state of flexible-grid optical networks refers to the occupancy of all the resources in the network and determines the network utilization and PLIs.

and compare three heuristic approaches for the RLP. Reference [11] proves the hardness of four different variants of the RLP and gives polynomial time and approximation algorithms.

Most of the previous works on the RLP have focused on minimizing the overall cost of RSs. In Refs. [7,8], the cost of individual traffic demand and the number of RSs are optimized in single-line-rate networks. Various heuristic approaches have also been proposed in Refs. [7,8] to reduce the total cost by allowing low-probability demands to have slightly costlier lightpaths. In Ref. [12], the RLP in waveband-switched networks is investigated, where the optimization objective is the combined cost of optical switch ports and regenerators.

The RLP studies mentioned above assume single-line-rate WDM networks. Multiple available modulation formats have also been considered in flexible-grid networks. The regenerator cost and spectrum usage are jointly optimized in a survivable network with different transponder profiles in Ref. [13], where the authors minimize the number of RSs subject to the constraint that each source–destination pair has two disjoint lightpaths. In Refs. [14,15], efficient heuristics and approximation algorithms are proposed to find RSs in mixed-line-rate networks with different reachabilities. The authors of [14,15] also show that certain network nodes are more likely to be selected as RSs through extensive simulations with various traffic profiles.

Most of the above works estimate PLIs based on transmission reach (TR) in fully loaded fiber links. Other models can also be used to predict QoTs and select RSs. In Ref. [16], the RLP in 10 Gbits/s non-return-to-zero on–off keying systems is solved based on an analytical expression of Q-factor combining various linear and nonlinear signal-degrading effects. Reference [17] allocates RSs jointly with routing, spectrum, and modulations using the Gaussian noise (GN) model [18–20] in dispersion-uncompensated flexible-grid networks. In this work, we also utilize the GN model to obtain accurate QoT estimations from the real-time and global resource allocation in the network.

All previous research into RLP assumes static traffic models where both the set of traffic demands and their data rates are fixed. Although the set of traffic demands remains relatively stable in the current backbone optical networks [21–23], the data rates of traffic demands will tend to be more dynamic and varying according to real-time requirements in the future [2,21]. Provided the flexible-grid-enabling BV-WXC and BV-T technologies [2] are utilized, customized transmission can be created in the network. Lightpaths can expand and contract their bandwidth according to the real-time traffic volume and user request. The corresponding optical channel bandwidths and the generated PLIs in the network will be random variables as well. Our work is different from previous research in that we consider a time-varying traffic scenario, where the stochastic PLIs are taken into account in the RLP.

In Ref. [24], we used the GN model and a modified statistical network assessment process (SNAP) framework [25–28] to perform Monte Carlo simulations and characterize the PLI empirically. Then a heuristic algorithm is proposed to allocate the RSs. The proposed method is compared with two previous algorithms [7,29] that are based on the TR model and static traffic prediction. This paper extends the work by (i) improving the heuristic in Ref. [24] with an optimization framework and providing a more detailed explanation of the algorithm, and (ii) presenting more results and analysis in the numerical simulations. The impact of data-rate-variable traffic on RS allocation is also studied.

The remainder of this paper is organized as follows: in Section II, the RLP in nonlinear flexible-grid networks with variable traffic is described. Our proposed algorithm is presented in Section III. Section IV presents and discusses numerical results. Section V concludes the paper.

II. Problem Statement

In this paper, we consider an optical network represented by a undirected graph with sets of nodes V and links E, where each link $l \in E$ is a bidirectional dispersion-uncompensated fiber link between nodes i and j for $i,j \in V$. The spectrum on each fiber is sliced into subcarriers with a bandwidth of b_{sub} each (in GHz). All traffic demands are assumed to use a uniform power spectral density (PSD) of G (in $\text{W} \cdot \text{THz}^{-1}$) and the same modulation format M with a spectral efficiency of c and a signal-to-noise ratio (SNR) threshold of SNR_{th} that guarantees an acceptable QoT. Note that it is also possible to assign different modulation formats for the lightpaths. This allows us to improve the spectrum utilization and reduce the number of RSs. On the other hand, the algorithms for allocating routing, spectrum, modulation formats, and RSs would be much more complicated. Therefore, to emphasize the impact of time-varying traffic in the RLP, we will not consider multiple modulation formats in this work. We require a guardband of bandwidth b_{sub} between any two adjacent channels. This requirement is ensured by assigning a guardband to the right side of each channel.

The set of traffic demands is denoted with T, where each element $t \in T$ is characterized by its pair of source s and destination t for $s \neq d$ and $s, d \in V$, and a date rate request R_t (in Gbps) including a forward error correction (FEC) overhead. We assume that the source–destination pairs in T are static and known, whereas the data rate requests are time-varying variables. A probability density function (PDF) $p_{R_t}(r_t)$ is used to represent its distribution. By employing Nyquist spectral shaping [30], the demand t with data rate r_t shows a bandwidth of $\Delta b_t = b_{\text{sub}} \cdot \lceil r_t/(b_{\text{sub}} \cdot c) \rceil$. The push–pull technique [31] and the dynamic lightpath adaptation algorithm [32,33] are used to adjust the bandwidth and shift the carrier frequencies of the optical channels without disruption. The spectrum ordering of demands is also assumed random, because the traffic loading process is usually unknown to the RLP, which is solved in the early stages of network planning, and the spectrum assignment will probably change after restorations from network failures. In response to the time-varying data rates and spectrum ordering, the transceivers and switches in the network are reconfigured periodically after fixed time intervals.

TABLE I
PARAMETERS IN THE PROBLEM STATEMENT

Parameter Type	Symbol	Meaning
Input	V	The set of nodes
	E	The set of links
	M	The name of the modulation format used in the network
	G	The PSD (in $\mathrm{W}\cdot\mathrm{THz}^{-1}$) used for all the traffic demands
	b_{sub}	The subcarrier bandwidth (in GHz) in the network
	c	The spectral efficiency of M
	$\mathrm{SNR}_{\mathrm{th}}$	The SNR threshold of M to achieve an acceptable QoT
	T	The set of traffic demands
	R_t	A random variable representing the data rate (in Gbps) of demand $t \in T$
	$p_{R_t}(r_t)$	The PDF of the data rate for demand $t \in T$
	Δb_t	The optical channel bandwidth (in GHz) of demand $t \in T$
	$F_{\max}$	The maximum number of RSs in the network
Output	$S(F_{\max})$	The set of output RSs whose total number is constrained by $F_{\max}$

As functions of data rates and spectrum ordering, the SNRs of traffic demands also vary with time. A blocking occurs when the temporary SNR of a demand is lower than $\mathrm{SNR}_{\mathrm{th}}$. To achieve efficient network operation, we assume that the temporarily blocked demands are still present in the network instead of being rejected and reconnected frequently. The noise blocking probability (BP) in this study is thus defined as the overall BP averaged over time. In this work, we assume that spectrum resources are sufficient to serve all the traffic demands in T. Therefore, blocking is only caused by a low QoT. This assumption allows us to mainly focus on the effect of time-varying traffic and RLP algorithms.

Based on the above-mentioned description, the parameters of our RLP are stated as follows and summarized in Table I:

1) *Input:* Network topology (V, E), subcarrier bandwidth b_{sub}, available modulation format M with spectral efficiency c, uniform PSD G, maximum number of RSs $F_{\max}$, and the set of data-rate-variable demands T with known $p_{R_t}(r_t)$ for $t \in T$.
2) *Output:* A set of RSs, denoted with $S(F_{\max})$, that minimizes the BP.

III. Regenerator Site Allocation Algorithm

The modified SNAP framework that simulates the PLI noise distributions for each demand–link pair is discussed in Section III.A. Then we present the RS allocation algorithm in Section III.B. The parameters used in this section are listed in Table II.

TABLE II
PARAMETERS IN THE PROPOSED ALGORITHM

Symbol	Meaning
P_t	The ordered set of links on the route of $t \in T$
Q_t	The ordered set of intermediate nodes on the route of $t \in T$
$\mathcal{L}(T)$	The ordered list of randomly shuffled demands in T
N_{MC}	The number of Monte Carlo repetitions
$N_{t,l}$	The random noise of the demand $t \in T$ on the link $l \in P_t$
$p_{N_{t,l}}(n)$	The PDF of $N_{t,l}$
f_i	A binary indicator that equals 1 if node $i \in V$ is an RS and 0 otherwise
$\mathbf{f}$	$\mathbf{f} = \{f_1, \ldots, f_{\lvert V\rvert}\}$ is a vector of f_i for $i \in V$
$H_t(\mathbf{f})$	The BP of the demand $t \in T$
$\mathtt{Seg}(t, \mathbf{f})$	The set of transparent segments on the route of the demand $t \in T$ that is divided by the RS allocation $\mathbf{f}$
$\mathtt{Seg}(t)$	The set of all possible transparent segments on the route of the demand $t \in T$
N_t^s	A random variable denoting the accumulated noise of the demand $t \in T$ at the end of the transparent segment $s \in \mathtt{Seg}(t)$
$p_{N_t^s}(n)$	The PDF of N_t^s
H_t^s	The BP of the demand $t \in T$ on the transparent segment $s \in \mathtt{Seg}(t)$
$\mathtt{src}(x)$	The source of x, where x can be a demand, link, or a transparent segment
$\mathtt{dst}(x)$	The destination of x, where x can be a demand, link, or a transparent segment
$\bar{V}_t$	$\bar{V}_t = \{\mathtt{src}(t), \mathtt{dst}(t)\} \cup Q_t$ for $t \in T$
w_s	The weight associated with the link $s \in \mathtt{Seg}(t)$
$\bar{D}_t$	The auxiliary weighted complete graph $\bar{D}_t = (\bar{V}_t, \mathtt{Seg}(t))$ with weight w_s for the link $s \in \mathtt{Seg}(t)$
$\mathcal{S}_t$	The set of promising RS allocations for $t \in T$
$\mathcal{S}_{t,k}$	The set of promising RS allocations with exactly k transparent segments for $t \in T$
K	The maximum number of different solutions that will be collected in $\mathcal{S}_{t,k}$
u_s	A binary variable that equals 1 if the transparent segment $s \in \mathtt{Seg}(t)$ has its source and destinations as RSs, the source, or the destination of $t \in T$ and 0 otherwise
u_s^κ	The value of u_s in the κ-th element of $\mathcal{S}_{t,k}$ for $\kappa \in \{1, \ldots, \lvert\mathcal{S}_{t,k}\rvert\}$
$\mathcal{U}_t$	$\mathcal{U}_t = \{1, \ldots, \lvert\mathcal{S}_t\rvert\}$, the set of indices for elements in $\mathcal{S}_t$
$\mathbf{f}^{t,\kappa}$	The κ-th element in $\mathcal{S}_t$ for $\kappa \in \mathcal{U}_t$
$y_{t,\kappa}$	The binary variable that equals 1 if the pre-calculated solution $\mathbf{f}^{t,\kappa} \in \mathcal{S}_t$ is chosen by the overall RS allocation, and 0 otherwise, $\kappa \in \mathcal{U}_t$
z_i	The binary variable that equals 1 if the node $i \in V$ is chosen by the overall RS allocation, and 0 otherwise
θ	A large enough real number

A. Modified Statistical Network Assessment Process

The incoherent GN model [18–20] is an analytical model to account for the nonlinear interference (NLI) caused by the Kerr effect. It takes the allocation of fiber links, spectral

orderings, and bandwidths of all the traffic demands as input and calculates the NLI noise for each demand–link pair $(t,l), \forall t \in T, l \in P_t$, where $P_t \subset |E$ denotes the ordered set of links on the route of t. The GN model is used by the SNAP framework to evaluate the NLI. Based on the GN model, the PLI noise is the sum of its NLI noise and the amplified spontaneous emission (ASE) noise introduced by optical amplifiers on its route. Therefore, under the condition that the data rates and spectrum orderings of all the demands in the network are random variables, the PLI noises for all the demand–link pairs are random variables as well. Despite the availability of more advanced strategies for optical power control [34–36], a uniform and fixed PSD is used for all the traffic demand in this work for the sake of simplicity. Note that in this work, we only take into account the most dominant and fundamental PLIs [19], whereas other signal quality degradation mechanisms such as optical crosstalk, filtering effect, and polarization-dependent loss are not included.

The probabilistic distribution of the PLI noise suffered by each demand–link pair is critical in quantifying the BP and achieving a robust regenerator placement. In this study, a modified version of the SNAP [25] is used to draw samples from the state space of the network and statistically characterize the PLI noise distributions. The flowchart of the modified SNAP is shown in Fig. 1.

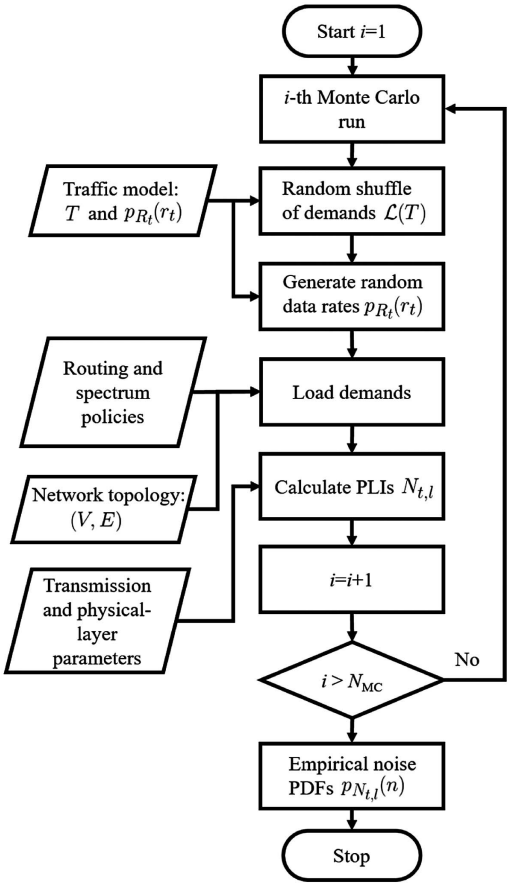

Fig. 1. Modified SNAP, which statistically characterizes PLI noise distributions.

The modified SNAP used in this study takes as input the following information:

1) The traffic model including the set of traffic demands T and the probabilistic distribution $p_{R_t}(r_t)$ for $t \in T$.
2) The routing and spectrum assignment policies.
3) The network topology (V, E).
4) Transmission and physical-layer parameters for PLI evaluation, i.e., the modulation format of optical signals, the PSD assignment policy, the fiber and optical amplifier parameters, etc.

The modified SNAP produces as output the PLI distributions for each demand–link pair by performing a Monte Carlo analysis. During each Monte Carlo run, a progressive load of the network is carried out to simulate one possible resource usage state of the network:

1) Shuffle the demands randomly and generate an ordered list of demands $\mathcal{L}(T)$.
2) Draw a random sample of the data rate from the PDF $p_{R_t}(r_t)$ for each $t \in T$.
3) Load demands with the order in $\mathcal{L}(T)$ and data rates are generated in step 2.
4) Calculate the PLI for each demand–link pair based on the GN model, the demand bandwidths, and the spectrum allocations from step 3.

Based on N_{MC} Monte Carlo repetitions, we can obtain an empirical PDF, $p_{N_{t,l}}(n)$, that describes the random noise $N_{t,l}$ for the demand t on the link l, for all $t \in T$ and $l \in P_t$.

B. RS Allocation Heuristic

By using the empirical PLI noise distributions generated from the modified SNAP simulations, the RLP heuristic minimizes the BP with a fixed number $F_{\max}$ of RSs. This is decomposed into two subproblems: 1) for each traffic demand, find a promising set of RS allocations, each of which is a subset of the global RS allocation offering a low BP for the demand; and 2) for each traffic demand, select one RS allocation scheme from its promising set of RS allocations calculated in step 1 such that the global RS allocation achieves a low BP and the number of RSs is no larger than $F_{\max}$.

We use $H_t(\mathbf{f})$ to denote the BP of demand $t \in T$ as a function of RS allocation $\mathbf{f}$ in the network, where $\mathbf{f}$ is a vector of f_i for all $i \in V$, and f_i is a binary indicator that equals 1 if node i is an RS and 0 otherwise. Suppose $\mathbf{f}$ divides the route of t into a set of transparent segments $\mathtt{Seg}(t,\mathbf{f})$. The evaluation of $H_t(\mathbf{f})$ for a given $\mathbf{f}$ is as follows:

1) Obtain $p_{N_t^s}(n)$, the PDF of the random accumulated PLI noise N_t^s at the end of the transparent segment $s \in \mathtt{Seg}(t,\mathbf{f})$, based on the simulation data in the modified SNAP. Here we have

$$N_t^s = \sum_{l \in s} N_{t,l} \tag{1}$$

and

$$p_{N_t^s}(n) = \underset{l \in s}{\otimes} p_{N_{t,l}}(n), \tag{2}$$

where the right-hand side of Eq. (2) is the convolution of all the $p_{N_{t,l}}(n)$ along s.

2) Calculate the BP H_t^s on the transparent segment s with

$$H_t^s = \int_{G/\mathrm{SNR_{th}}}^{+\infty} p_{N_t^s}(n)\mathrm{d}n. \tag{3}$$

3) Calculate $H_t(\mathbf{f})$ under the assumption that the BPs on disjoint transparent segments are independent by using

$$H_t(\mathbf{f}) = 1 - \Pi_{s \in \mathrm{Seg}(t,\mathbf{f})}(1 - H_t^s), \tag{4}$$

or, equivalently,

$$-\ln(1 - H_t(\mathbf{f})) = -\sum_{s \in \mathrm{Seg}(t,\mathbf{f})} \ln(1 - H_t^s). \tag{5}$$

To obtain the promising set of RS allocations that contains the optimal solution for the demand t, we first calculate H_t^s for all $s \in \mathtt{Seg}(t)$, where $\mathtt{Seg}(t)$ is the set of all possible transparent segments on the route of t. Then we construct a weighted directed graph $\bar{D}_t = (\bar{V}_t, \mathtt{Seg}(t))$. The set of nodes in $\bar{D}_t$ is $\bar{V}_t = \{\mathtt{src}(t), \mathtt{dst}(t)\} \cup Q_t$, which contains all the network nodes along the route of t, including its source and destination. The set of links in $\bar{D}_t$ is $\mathtt{Seg}(t)$, which contains all the transparent segments connecting any pair of nodes along the route of t. The weight w_s associated with the link $s \in \mathtt{Seg}(t)$ in $\bar{D}_t$ is

$$w_s = \begin{cases} -\ln(1 - H_t^s), & \text{if } H_t^s < 1, \\ +\infty, & \text{if } H_t^s = 1. \end{cases} \tag{6}$$

In $\bar{D}_t$, the set of nodes on a path between $\mathtt{src}(t)$ and $\mathtt{dst}(t)$ is equivalent to an RS allocation on the route of t, and the total path weight corresponds to the BP of the RS allocation according to Eq. (5). This transformation from an RS allocation and its corresponding BP to a weighted route in $\bar{D}_t$ facilitates the search for promising RS allocations. We identify the promising set of RS allocations with $k-1$ RSs by an exhaustive search of the K-shortest weighted paths in $\bar{D}_t$ with k transparent segments. This search is summarized in Algorithm 1 where steps 3–12 are repeated for different values of k. Specifically, we search for the K-shortest paths in $\bar{D}_t$ with path lengths of k. For each k, Eq. (7) is solved iteratively to find K different solutions, which corresponds to steps 4–10 in Algorithm 1:

$$\underset{u_s}{\text{minimize}} \sum_{s \in \mathrm{Seg}(t)} w_s u_s, \tag{7a}$$

$$\text{subject to} \sum_{\substack{s \in \mathrm{Seg}(t) \\ \mathtt{src}(s) = i}} u_s - \sum_{\substack{s \in \mathrm{Seg}(t) \\ \mathtt{dst}(s) = i}} u_s = \begin{cases} 1, & \text{if } i = \mathtt{src}(t), \\ -1, & \text{if } i = \mathtt{dst}(t), \\ 0, & \text{otherwise}, \end{cases} \quad \forall i \in \bar{V}, \tag{7b}$$

$$\sum_{s \in \mathrm{Seg}(t)} u_s = k, \tag{7c}$$

$$\sum_{\substack{s \in \mathrm{Seg}(t) \\ u_s^\kappa = 1}} u_s \le k - 1, \quad \forall \kappa \in \{1, \ldots, |\mathcal{S}_{t,k}|\}. \tag{7d}$$

Here u_s for $s \in \mathtt{Seg}(t)$ is a binary variable that equals 1 if the transparent segment s has its two endpoints as RSs, source, or destination of t, and 0 otherwise. $S_{t,k}$ is the set of solutions obtained at previous iterations of solving Eq. (7) with k transparent segments. u_s^κ is the value of u_s in the κ-th element of $\mathcal{S}_{t,k}$ for $\kappa \in \{1, \ldots, |\mathcal{S}_{t,k}|\}$. The objective (7a) calculates the BP of the demand t. Equation (7b) is the flow conservation constraint. Specifically, Eq. (7b) states the following three possible cases for a node: 1) it has only one outgoing link if it is the source of a path; 2) it has only one incoming link if it is the destination of a path; and 3) it has one outgoing as well as one incoming link if it is an intermediate node of a path. Equation (7c) is a constraint on the number of transparent segments. In Eq. (7d), inequality searches for new solutions by excluding those already found. In other words, it requires that the current solution does not have all 1 s at the same positions as in previous solutions. Hence, a different solution is obtained by adding Eq. (7d).

Algorithm 1: Search of potential RS allocations for $t, t \in T$

Input:
- The weighted complete graph $\bar{D}_t = (\bar{V}, \mathtt{Seg}(t))$ with link weights specified in Eq. (6).
- A constant K giving the number of RS solutions with the same number of transparent segments that will be searched

1: Let $\mathcal{S}_t$ denote the set of promising RS allocations
2: Initialize $\mathcal{S}_t = \varnothing$
3: **for** k in $\{1, \ldots, |Q_t|\}$ **do**
4: Let $\mathcal{S}_{t,k}$ denote the set of RS allocations with exactly k RSs
5: Initialize $\mathcal{S}_{t,k} = \varnothing$
6: **for** j in $\{1, \ldots, K\}$ **do**
7: Solve (7) and convert its solution and objective value to an RS allocation $\mathbf{f}$ and the BP $H_t(\mathbf{f})$, respectively
8: Update (7) by adding the new solution to (7d)
9: $\mathcal{S}_{t,k} \leftarrow \mathcal{S}_{t,k} \cup \{\mathbf{f}\}$
10: **end for**
11: $\mathcal{S}_t \leftarrow \mathcal{S}_t \cup \mathcal{S}_{t,k}$
12: **end for**

Output: The set of all potential paths $\mathcal{S}_t$ and the corresponding noise blocking probability $H_t(\mathbf{f}), \forall \mathbf{f} \in \mathcal{S}_t$

As described by step 7 of Algorithm 1, after Eq. (7) has been solved, its solution u_s and the objective value $\sum_{s \in \mathrm{Seg}(t)} w_s u_s$ are converted to an RS allocation $\mathbf{f}$ and the BP $H_t(\mathbf{f})$, respectively. Based on the sets of promising RS allocations $\mathcal{S}_t$ for the demand $t \in T$, we can select the overall RS allocation that satisfies the constraint on the number of RSs and achieves the minimum BP by solving the optimization problem:

$$\underset{y_{t,\kappa},z_i}{\text{minimize}} \sum_{t\in T}\sum_{\kappa\in\mathcal{U}_t} y_{t,\kappa}H(\mathbf{f}^{t,\kappa}), \tag{8a}$$

$$\text{subject to} \sum_{\kappa\in\mathcal{U}_t} y_{t,\kappa} = 1, \quad \forall t \in T, \tag{8b}$$

$$\sum_{t\in T}\sum_{\kappa\in\mathcal{U}_t} f_i^{t,\kappa} y_{t,\kappa} \le \theta z_i, \quad \forall i \in V, \tag{8c}$$

$$\sum_{i\in V} z_i \le F_{\max}. \tag{8d}$$

Here $\mathcal{U}_t = \{1, \ldots, |\mathcal{S}_t|\}$ is the set of indices for elements in $\mathcal{S}_t$; the binary variable $y_{t,\kappa}$ indicates if the pre-calculated solution $\mathbf{f}^{t,\kappa} \in \mathcal{S}_t$ is selected into the final RS allocation; the binary variable z_i indicates if the node $i \in V$ is chosen as an RS; $f_i^{t,\kappa}$ is the ith element of $\mathbf{f}^{t,\kappa}$; θ is a large enough number; and $F_{\max}$ is the maximum number of RSs in the network. To ensure a valid binary variable z_i, the value of θ should be greater than the maximum of the left-hand side in Eq. (8c), whose upper bound is derived as follows

$$\sum_{t\in T}\sum_{\kappa\in\mathcal{U}_t} f_i^{t,\kappa} < \sum_{t\in T}\sum_{\kappa\in\mathcal{U}_t} 1 < \sum_{t\in T} |Q_t|K < |T||V|K.$$

The last two inequalities hold because $|\mathcal{U}_t| < |Q_t|K$ and $|Q_t| < |V|$. Therefore, we can set θ to $|T||V|K$ in Eq. (8c). The objective (8a) calculates the overall BP in the network; Eq. (8b) implies that exactly one RS allocation from $\mathcal{S}_t$ is chosen for each demand $t \in T$; Eq. (8c) is used to calculate whether a node is selected as an RS for each node; and Eq. (8d) is the constraint on the number of RSs.

The complexity of the proposed method is mainly attributed to the modified SNAP, whose required computational resources grow proportionally with the number of simulations N_{MC}. The RS allocation heuristic, however, has a comparatively low computational complexity due to the relatively simple formulations in Eqs. (7) and (8), as measured by the number of variables involved.

IV. Numerical Results

In this section, we present simulation results for the proposed RS allocation heuristic. We first verify the accuracy of our BP estimation by the objective of Eq. (8) against simulation results. Next, we study the impact of data-rate-variable traffic demands on BP, then compare it with two previous algorithms [7,29] based on the TR model and static traffic prediction. The first benchmark is the greedy constrained-routing RLP (greedy CRLP) [7] that minimizes the number of RSs subject to certain routing constraint (in most cases, it is the shortest path constraint), a static traffic matrix, and a provided TR. The second benchmark is the routing and reach heuristic (RR) [29] that ranks the likelihood of being an RS for each node based on the network connectivity and TR model. This likelihood rank of nodes can also be obtained with the proposed algorithm by varying the value of $F_{\max}$ and recording the increment of $S(F_{\max})$. The BP and node ranking performance of the proposed algorithm are studied against the greedy CRLP and RR, respectively, in the data-rate-variable scenario with the same TRs.

The continental U.S. topology (CONUS) with 75 nodes and 99 bidirectional links, shown in Fig. 2, is studied in the numerical simulations. We assume that there is one traffic demand between each node pair. The shortest-distance routes and the first-fit spectrum allocation scheme are used for all the traffic demands. BV-Ts with a single modulation format of polarization-multiplexing quadrature phase shift keying with Nyquist spectral shaping are applied to all the traffic demands to obtain a spectral efficiency of 4 bits/s/Hz for a raw channel data rate including the FEC overhead. A uniform and fixed PSD of $G = 15$ mW/THz is applied to all the traffic demands. The subcarrier bandwidth on all the fiber links is $b_{\text{sub}} = 12.5$ GHz. The demand data rate R_t is assumed to follow a normal distribution, i.e., $R_t \sim N(\mu, \sigma^2)$, for all the demands $t \in T$, with $\mu = 200$ Gbps and $\sigma = 20$ Gbps. We consider a standard single-mode fiber with the following characteristics: loss coefficient $\alpha = 0.22$ dB/km, dispersion coefficient $D = 16.7$ ps/nm/km, nonlinear coefficient $\gamma = 1.32 \times 10^{-3}$ $(\text{Wm})^{-1}$. The noise figure of the erbium-doped fiber amplifier is 5.5 dB. The span length is uniformly 100 km across the network.

In the modified SNAP, $N_{\text{MC}} = 7 \times 10^4$ sets of random traffic are used to simulate the PLI noise distributions $p_{N_{t,l}}$. For performance verification, 3×10^4 sets of random traffic with shuffled spectrum orderings are used to simulate the BP. This gives a BP resolution of 3.3×10^{-5}, which corresponds to on average one noise blocking per demand in the whole BP simulation. Also observe that the accuracy of the PLI distribution output by the modified SNAP is dependable up to a certain confidence level. Therefore, the accuracy of the BP simulation as well as the PLI noise distributions can be improved by increasing the number of simulated traffic matrices in both parts.

Note that the benchmarks require the TR value as input, which is determined by the SNR threshold of the chosen transmission scheme and the fiber and amplifier parameters. To make a thorough comparison with the benchmarks in all possible cases, we vary the TR value from 1300 to 5000 km by scaling the SNR threshold proportionally, which corresponds to different coding schemes and error-correction capacities. Specifically, when scaling the SNR

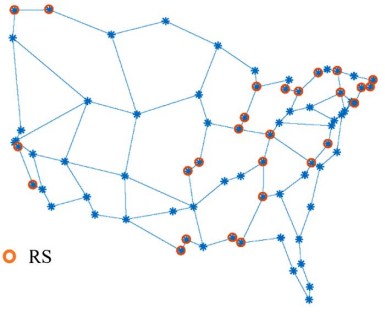

Fig. 2. CONUS network topology. The circles represent an example RS allocation.

threshold, its multiplication with TR is a constant given by $\mathrm{SNR}_{\mathrm{th}} \times \mathrm{TR} = \mathrm{const}$. A few examples of the mapping between SNR thresholds and TRs in our simulations are shown in Table III. Moreover, the simulation results over different TR values can also help us to understand in what transmission scenarios the proposed algorithm is effective. Observe that in the method proposed by us, the TR values, or, equivalently, the SNR thresholds, are used in Eq. (3) to represent how much PLI noise a traffic demand can sustain without being blocking, whereas the GN model is still used to calculate the actual PLIs.

BP estimation accuracy: The BPs predicted by Eq. (8) are compared with the simulation results in Fig. 3 for different TR values. The BPs are shown as functions of the number of RSs. The simulated and predicted BPs are close to each other, which means that the modified SNAP can empirically depict the PLI distributions well. The simulated curves have slightly higher BPs than the predicted ones. This is because the results of the proposed algorithm are based on the empirical PLI distributions obtained in the modified SNAP. Due to the limited number of simulations, there is still a slight discrepancy between the empirical and true PLI distributions. Therefore, the predictions based on the empirical PLI distributions are not the same as the simulated ones. The difference between the two curves will converge to zero as we increase N_{MC}, the number of Monte Carlo simulations in SNAP.

Impact of data-rate-variable traffic: Figure 4 illustrates the impact of a variable data rate by simulating the BPs of demands with zero standard deviation. The RS allocations are based on the traffic with $\sigma = 20$ Gbps. A larger variance causes stronger PLIs for some of the demands and results in higher overall BPs. The zero-variance traffic has less randomness in the PLI noise and, thus, has lower BPs. Therefore, it is necessary to consider the variable traffic in the RLP in nonlinear flexible-grid networks.

TABLE III
MAPPING BETWEEN SNR THRESHOLDS AND TRS

SNR Threshold	TR (km)
14.60	1300
9.49	2000
7.03	2700
5.58	3400

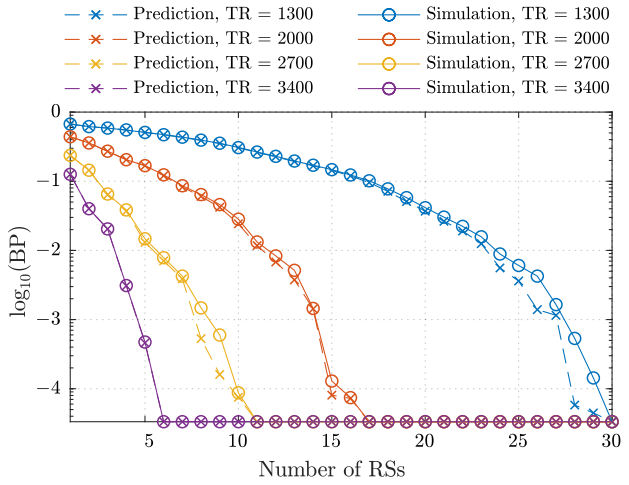

Fig. 3. BPs of the prediction and simulation with different TRs.

Comparison with the greedy CRLP: In Fig. 5, the required numbers of RSs to achieve the same level of BPs at different TRs are compared for both the proposed algorithm and the greedy CRLP. At each TR, the greedy CRLP computes one RS set and its corresponding BP, whereas the proposed algorithm can generate multiple RS sets, each for a different F_{max}. To make a comparison between the two methods, we sweep F_{max} and choose the smallest one that achieves a BP no larger than that of the greedy CRLP. As shown in Fig. 5, the proposed algorithm requires fewer RSs than the greedy CRLP for most of the TRs. The average reduction in the number of RSs is around 10%.

Overprovision of the TR model: To study the impact of the PLI models in the RLP, we analyze the PLI PSD of the demand with the highest impairments on each link calculated by the GN model, which is normalized to the worst

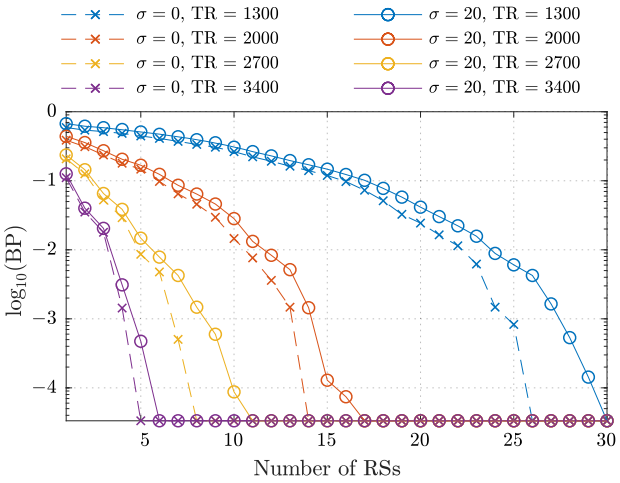

Fig. 4. Simulated BPs for traffic demands with different standard deviations of data rates.

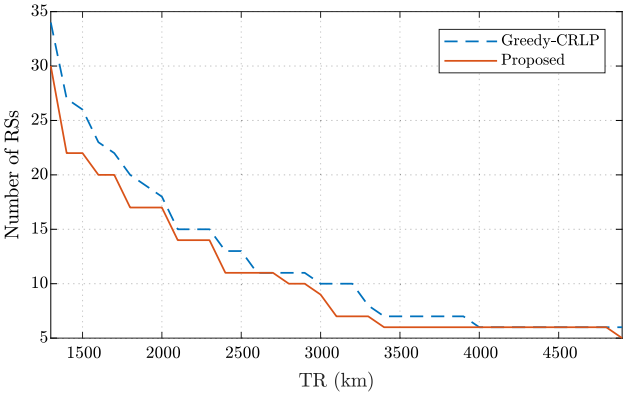

Fig. 5. Number of RSs required by the proposed and greedy CRLP algorithms to achieve similar BPs.

case PLI noise estimated by the TR model. The means and standard deviations of the normalized noise are plotted in Fig. 6. We observe that the TR model tends to overestimate the PLIs, which leads to an inefficient placement of RSs. This is because the TR model assumes that all the links are fully occupied, which is not the case in the network scenario due to the inevitable spectrum segmentation and geographical distribution of traffic.

Comparison with the RR: We compare the node ranking of being an RS as calculated by the proposed method and the RR method by visualizing their resulting BPs in Fig. 7. The BPs of different TRs are plotted as functions of the number of RSs for both methods. In the RR method, a node gets a higher rank if it is chosen as an RS by more traffic demands. As a result, two highly ranked nodes in the RR can be used to serve similar demands and are not necessary to be RSs at the same time. If we select both of them as RSs, the BP will not gain much but the RS resources are wasted. This is the reason for the plateau areas in the RR curves in Fig. 7. In contrast, by optimizing the RS in combination instead of individually based on the empirical PLI distributions,

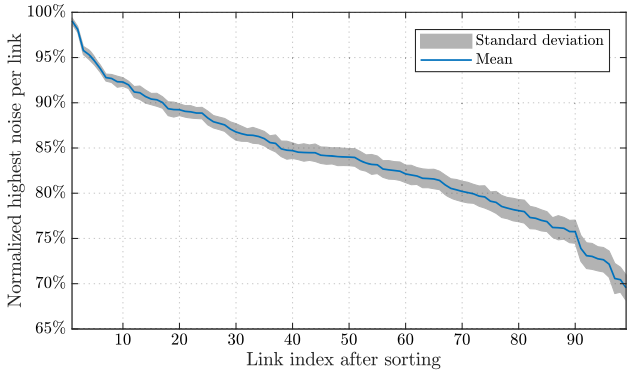

Fig. 6. Highest PLI noise per link from the GN model normalized to the worst case from the TR model. The link indices are sorted in such a way that the means are in a descending order.

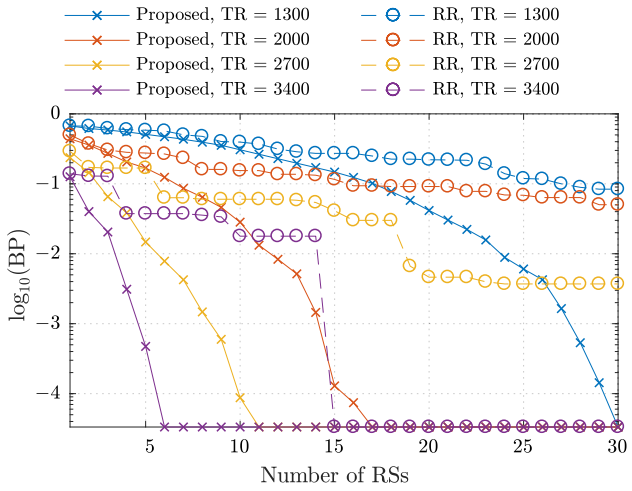

Fig. 7. BPs of the proposed and RR methods for different TRs and numbers of RSs.

the proposed algorithm achieves significantly lower BPs compared with the RR, with an average BP gain of two orders of magnitude.

V. Conclusion

The paper tackles the RLP in nonlinear flexible-grid networks with variable data rate requests. The GN model and the modified SNAP framework are applied to statistically describe the PLI noise distribution of each demand–link pair in the network, based on which the set of RSs are determined. The proposed method also predicts the BP performance of its solution with an accuracy of up to 3.3×10^{-5}. The efficiency of the allocated RS set is improved by 10% compared with that in the greedy CRLP algorithm, by estimating the PLI more accurately and taking into account the realistic traffic conditions in the network.

Acknowledgment

This research is supported in part by the NSF Grant CCF-1422871, the Swedish Research Council Grant 2012-5280, and the Ericsson Research Foundation.

References

[1] O. Gerstel, M. Jinno, A. Lord, and S. Yoo, "Elastic optical networking: a new dawn for the optical layer?" *IEEE Commun. Mag.*, vol. 50, no. 2, pp. s12–s20, 2012.

[2] M. Jinno, H. Takara, B. Kozicki, Y. Tsukishima, Y. Sone, and S. Matsuoka, "Spectrum-efficient and scalable elastic optical path network: architecture, benefits, and enabling technologies," *IEEE Commun. Mag.*, vol. 47, no. 11, pp. 66–73, 2009.

[3] M. Klinkowski, M. Ruiz, L. Velasco, D. Careglio, V. Lopez, and J. Comellas, "Elastic spectrum allocation for time-varying traffic in flexgrid optical networks," *IEEE J. Sel. Areas Commun.*, vol. 31, no. 1, pp. 26–38, 2013.

[4] L. Beygi, E. Agrell, J. M. Kahn, and M. Karlsson, "Rate-adaptive coded modulation for fiber-optic communications," *J. Lightwave Technol.*, vol. 32, no. 2, pp. 333–343, 2014.

[5] N. Sambo, G. Meloni, F. Cugini, A. D'Errico, L. Pot, P. Iovanna, and P. Castoldi, "Routing code and spectrum assignment (RCSA) in elastic optical networks," *J. Lightwave Technol.*, vol. 33, no. 24, pp. 5114–5121, 2015.

[6] J. Zhao, L. Yan, H. Wymeersch, and E. Agrell, "Code rate optimization in elastic optical networks," in *European Conf. Optical Communication (ECOC)*, Valencia, Spain, Sept. 2015, paper We.3.5.1.

[7] B. G. Bathula, R. K. Sinha, A. L. Chiu, M. D. Feuer, G. Li, S. L. Woodward, W. Zhang, R. Doverspike, P. Magill, and K. Bergman, "Constraint routing and regenerator site concentration in ROADM networks," *J. Opt. Commun. Netw.*, vol. 5, no. 11, pp. 1202–1214, 2013.

[8] B. G. Bathula, A. L. Chiu, R. K. Sinha, and S. L. Woodward, "Routing and regenerator planning in a carrier's core ROADM network," in *Optical Fiber Communication Conf. (OFC)*, Los Angeles, CA, Mar. 2017, paper Th4F.4.

[9] S. Chen, I. Ljubić, and S. Raghavan, "The regenerator location problem," *Networks*, vol. 55, no. 3, pp. 205–220, 2010.

[10] B. G. Bathula, R. K. Sinha, A. L. Chiu, M. D. Feuer, G. Li, S. L. Woodward, W. Zhang, R. Doverspike, P. Magill, and

K. Bergman, "Cost optimization using regenerator site concentration and routing in ROADM networks," in *IEEE Int. Conf. Design of Reliable Communication Networks (DRCN)*, Budapest, Hungary, Mar. 2013, pp. 139–147.

[11] M. Flammini, A. Marchetti-Spaccamela, G. Monaco, L. Moscardelli, and S. Zaks, "On the complexity of the regenerator placement problem in optical networks," *IEEE/ACM Trans. Netw.*, vol. 19, no. 2, pp. 498–511, 2011.

[12] S. Varma and J. P. Jue, "Regenerator placement and waveband routing in optical networks with impairment constraints," in *Int. Conf. Communications (ICC)*, Kyoto, Japan, 2011, paper ONSP–1.

[13] A. Eira, J. Santos, J. Pedro, and J. Pires, "Design of survivable flexible-grid DWDM networks with joint minimization of transponder cost and spectrum usage," in *European Conf. Optical Communication (ECOC)*, Amsterdam, the Netherlands, Sept. 2012, paper P5.16.

[14] W. Xie, J. P. Jue, X. Wang, Q. Zhang, Q. She, P. Palacharla, and M. Sekiya, "Regenerator site selection for mixed line rate optical networks," *J. Opt. Commun. Netw.*, vol. 6, no. 3, pp. 291–302, 2014.

[15] W. Xie, J. P. Jue, X. Wang, Q. Zhang, Q. She, P. Palacharla, and M. Sekiya, "Cost-optimized design of flexible-grid optical networks considering regenerator site selection," in *IEEE Global Communications Conf. (GLOBECOM)*, Atlanta, GA, Dec. 2013, pp. 2358–2363.

[16] S. Pachnicke, T. Paschenda, and P. Krummrich, "Assessment of a constraint-based routing algorithm for translucent 10Gbits/s DWDM networks considering fiber nonlinearities," *J. Opt. Netw.*, vol. 7, no. 4, pp. 365–377, 2008.

[17] N. Dharmaweera, L. Yan, J. Zhao, M. Karlsson, and E. Agrell, "Regenerator site selection in impairment-aware elastic optical networks," in *Optical Fiber Communication Conf. (OFC)*, Anaheim, CA, Mar. 2016, paper Tu3F.1.

[18] P. Poggiolini, G. Bosco, A. Carena, V. Curri, Y. Jiang, and F. Forghieri, "The GN-model of fiber non-linear propagation and its applications," *J. Lightwave Technol.*, vol. 32, no. 4, pp. 694–721, 2014.

[19] P. Johannisson and E. Agrell, "Modeling of nonlinear signal distortion in fiber-optic networks," *J. Lightwave Technol.*, vol. 32, no. 23, pp. 4544–4552, 2014.

[20] L. Yan, E. Agrell, H. Wymeersch, and M. Brandt-Pearce, "Resource allocation for flexible-grid optical networks with nonlinear channel model," *J. Opt. Commun. Netw.*, vol. 7, no. 11, pp. B101–B108, 2015.

[21] E. Agrell, M. Karlsson, A. Chraplyvy, D. J. Richardson, P. M. Krummrich, P. Winzer, K. Roberts, J. K. Fischer, S. J. Savory, B. J. Eggleton, and M. Secondini, "Roadmap of optical communications," *J. Opt.*, vol. 18, no. 6, 063002, 2016.

[22] A. Leiva, C. M. Machuca, A. Beghelli, and R. Olivares, "Migration cost analysis for upgrading WDM networks," *IEEE Commun. Mag.*, vol. 51, no. 11, pp. 87–93, 2013.

[23] A. Zapata-Beghelli and P. Bayvel, "Dynamic versus static wavelength-routed optical networks," *J. Lightwave Technol.*, vol. 26, no. 20, pp. 3403–3415, 2008.

[24] L. Yan, Y. Xu, M. Brandt-Pearce, N. Dharmaweera, and E. Agrell, "Regenerator allocation in nonlinear elastic optical networks with random data rates," in *Optical Fiber Communication Conf. (OFC)*, San Diego, CA, Mar. 2018, paper Th2A.47.

[25] M. Cantono, R. Gaudino, and V. Curri, "Potentialities and criticalities of flexible-rate transponders in DWDM networks: a statistical approach," *J. Opt. Commun. Netw.*, vol. 8, no. 7, pp. A76–A85, 2016.

[26] V. Curri, M. Cantono, and R. Gaudino, "Elastic all-optical networks: a new paradigm enabled by the physical layer. How to optimize network performances?" *J. Lightwave Technol.*, vol. 35, no. 6, pp. 1211–1221, 2017.

[27] M. Cantono, R. Gaudino, P. Poggiolini, and V. Curri, "Comparing networking benefits of digital back-propagation vs. lightpath regeneration," in *European Conf. Optical Communication (ECOC)*, Düsseldorf, Germany, Sept. 2016, paper Tu.3.D.4.

[28] M. Cantono and V. Curri, "Flex- vs. fix-grid merit in progressive loading of networks already carrying legacy traffic," in *Int. Conf. Transparent Optical Networks (ICTON)*, Girona, Spain, July 2017, paper Th.B4.5.

[29] J. Pedro, "Predeployment of regenerators for fast service provisioning in DWDM transport networks," *J. Opt. Commun. Netw.*, vol. 7, no. 2, pp. A190–A199, 2015.

[30] R. Schmogrow, M. Winter, M. Meyer, D. Hillerkuss, S. Wolf, B. Baeuerle, A. Ludwig, B. Nebendahl, S. Ben-Ezra, J. Meyer, M. Dreschmann, M. Huebner, J. Becker, C. Koos, W. Freude, and J. Leuthold, "Real-time Nyquist pulse generation beyond 100 Gbit/s and its relation to OFDM," *Opt. Express*, vol. 20, no. 1, pp. 317–337, 2012.

[31] F. Cugini, F. Paolucci, G. Meloni, G. Berrettini, M. Secondini, F. Fresi, N. Sambo, L. Poti, and P. Castoldi, "Push-pull defragmentation without traffic disruption in flexible grid optical networks," *J. Lightwave Technol.*, vol. 31, no. 1, pp. 125–133, 2013.

[32] A. Asensio, M. Klinkowski, M. Ruiz, V. López, A. Castro, L. Velasco, and J. Comellas, "Impact of aggregation level on the performance of dynamic lightpath adaptation under time-varying traffic," in *IEEE Int. Conf. Optical Network Design and Modeling (ONDM)*, Brest, France, Apr. 2013, pp. 184–189.

[33] L. Velasco, A. P. Vela, F. Morales, and M. Ruiz, "Designing, operating, and reoptimizing elastic optical networks," *J. Lightwave Technol.*, vol. 35, no. 3, pp. 513–526, 2017.

[34] P. Poggiolini, G. Bosco, A. Carena, R. Cigliutti, V. Curri, F. Forghieri, R. Pastorelli, and S. Piciaccia, "The LOGON strategy for low-complexity control plane implementation in new-generation flexible networks," in *Optical Fiber Communication Conf. (OFC)*, Anaheim, CA, Mar. 2013, paper OW1H.3.

[35] R. Pastorelli, S. Piciaccia, G. Galimberti, E. Self, M. Brunella, G. Calabretta, F. Forghieri, D. Siracusa, A. Zanardi, E. Salvadori, G. Bosco, A. Carena, V. Curri, and P. Poggiolini, "Optical control plane based on an analytical model of nonlinear transmission effects in a self-optimized network," in *European Conf. Optical Communication (ECOC)*, London, UK, Sept. 2013, paper We.3.E.4.

[36] V. Curri, A. Carena, A. Arduino, G. Bosco, P. Poggiolini, A. Nespola, and F. Forghieri, "Design strategies and merit of system parameters for uniform uncompensated links supporting Nyquist-WDM transmission," *J. Lightwave Technol.*, vol. 33, no. 18, pp. 3921–3932, 2015.